Photoconductivity in insulating $YBa_2Cu_3O_{6+x}$: From Mott-Hubbard insulator to Fermi glass via oxygen doping

G. Yu, C. H. Lee, D. Mihailovic,* and A. J. Heeger
Institute for Polymers and Organic Solids and Department of Physics, University of California at Santa Barbara, Santa Barbara, California 93106

C. Fincher, N. Herron, and E. M. McCarron
E. I. du Pont de Nemours and Co., Inc., Central Research and Development Department, Wilmington, Delaware 19898
(Received 14 December 1992; revised manuscript received 1 June 1993)

Photoconductivity, $\sigma_{ph}(\omega)$, and optical conductivity, $\sigma(\omega)$, are compared for insulating $YBa_2Cu_3O_{6+x}$ ($x<0.4$) in the photon energy range from 0.6 to 3.3 eV. With $x\approx 0$, there is an energy gap with weak spectral features at 1.5 and 2.1 eV, in addition to the well-known 1.75 and 2.7 eV bands. The coincidence between $\sigma_{ph}(\omega)$ and $\sigma(\omega)$ at the band edge implies the photogeneration of separated charge carriers; no significant exciton binding energy is observed. The spectral gap in stoichiometric $YBa_2Cu_3O_6$ is consistent with the electronic structure of a Mott-Hubbard insulator with a well-defined energy gap between the filled O $2p$ band and the empty Cu $3d$ upper Hubbard band. The 1.5-eV feature determines the lowest-energy interband transition. Oxygen doping into the O(1) sites results in a major change in electronic structure. For $x\approx 0.3$, the absorption observed throughout the infrared has no counterpart in $\sigma_{ph}(\omega)$; the photoconductivity turns on near 2 eV. In addition, thermally activated behavior is observed for the 1.75-eV band in $\sigma_{ph}(\omega)$. We conclude that upon doping, the states involved in transitions below 2 eV become localized. The data imply that the random distribution of oxygen ions at O(1) sites causes a change of electronic structure from a Mott-Hubbard insulator with a well-defined interband charge-transfer energy gap (at $x=0$) to a Fermi glass (at $x\approx 0.3$).

I. INTRODUCTION

Studies of the changes in electronic structure of the high-temperature superconducting (HTSC) cuprates as a function of chemical doping are of fundamental importance for understanding of the mechanism of high-T_c superconductivity. For this reason, the optical properties of $YBa_2Ca_3O_{6+x}$ have been widely studied; measurements by means of reflectivity, ellipsometry, resonant Raman scattering, and photoemission have provided a wealth of information on the complex dielectric function and the band structure.[1-7] Nevertheless, there is only limited understanding of the electronic structure of this important HTSC material.

Although band calculations using the linear muffin-tin orbital method in the local-density approximation can explain a variety of data in metallic and/or superconducting $YBa_2Cu_3O_7$ (for example, based upon Raman scattering, photoemission, and neutron-scattering results, a Fermi energy diagram has been constructed),[7-9] band theory fails to explain the antiferromagnetic and insulating ground state[10] of $YBa_2Cu_3O_6$, which is generally regarded as a strongly correlated Mott-Hubbard insulator. Doping, by addition of oxygen to the O(1) sites, introduces carriers and simultaneously introduces disorder. The fact that the system remains insulating even at high-carrier concentrations (e.g., $x\approx 0.4$, where the carrier density should be of order 10^{21} cm^{-3}), suggests that at intermediate x the system should be described in terms of disorder-induced localization, i.e., a Fermi glass. This conclusion would imply that as x is increased from 0 to 1, $YBa_2Cu_3O_{6+x}$ evolves from an insulator with a well-defined energy gap to a Fermi glass, and then through a metal-insulator transition to a metal. In this study, we utilize a combination of optical and photoconductivity data to address the evolution of $YBa_2Cu_3O_{6+x}$ from a Mott-Hubbard insulator to a Fermi glass via oxygen doping.

In ceramic and crystalline $YBa_2Cu_3O_{6+x}$ with x near zero, the optical conductivity, $\sigma(\omega)$, shows three major features, at 1.75, 2.7, and 4.2 eV.[2] Upon doping with oxygen, a broad absorption band grows across the mid-infrared spectral region, accompanied by a reduction of oscillation strength above the charge-transfer (CT) gap.[1,3] No major changes in the mid-ir absorption are found in association with the metal-insulator (MI) transition, which occurs at $x\approx 0.4$. Rather, this subgap absorption is observed at very low doping concentrations (as soon as carriers are added to the CuO_2 layers) and increases in strength monotonically across the MI transition boundary into the metallic and/or superconducting phase.[11] The oscillator strength of the ir absorption increases with doping concentration, while the shape of the broad spectral feature is insensitive to the doping level.[3]

Transient photoinduced conductivity[12-14] data obtained from single crystals of $YBa_2Cu_3O_{6+x}$ and $La_2CuO_{4+\delta}$, and transport data[15,16] obtained from single crystals of $Nd_{2-x}Ce_xCuO_4$ and $Bi_2Sr_2Ca_{1-x}Y_xCu_2O_8$, have provided evidence that the MI transition is dominated by disorder-induced localization. The transition

results from shifting the Fermi level (E_F) from the region of localized electronic states across the mobility edge (E_c) into the region of extended states by varying the carrier density of the CuO_2 planes either by chemical doping or by photoexcitation. The temperature dependence of the resistivity in insulating cuprates (single-crystal samples) is thermally activated at high temperatures and dominated by hopping conduction at low temperatures,[14–18] a combination which is consistent with the electronic structure of a Fermi glass. The Hall coefficient,[17,18] ac conductivity,[19–22] and thermopower[23] data, obtained from the insulating phase of partially doped cuprates, also support the Fermi glass description of the electronic structure, i.e., the insulating state results from the localization of the electronic wave functions at E_F, rather than from a gap in the electronic density of states at the Fermi energy.

Although one would like to study these doping-induced changes in electronic structure spectroscopically, one cannot distinguish from optical data alone whether the initial and/or the final states in an optical transition are extended or localized, nor can one distinguish whether the resulting excitations are charged or neutral. To make such distinctions requires a comparison of the photoconductive response, $\sigma_{ph}(\omega)$, with the optical conductivity, $\sigma(\omega)$. Early observations have shown that in partially doped single crystals of $YBa_2Cu_3O_{6+x}$ (with $x \approx 0.3$), $\sigma_{ph}(\omega)$ drops rapidly for energies below 2 eV while $\sigma(\omega)$ remains large throughout the ir. The absorption below 2 eV does not contribute to the photoconductivity.[24]

To address the doping-induced changes in electronic structure, we report and compare $\sigma_{ph}(\omega)$ and $\sigma(\omega)$ in the photon energy range from 0.6 to 3.3 eV. With $x \approx 0$, weak spectral features are observed at 1.5 and 2.1 eV, in addition to the well-known 1.75 and 2.7 eV bands. The coincidence between $\sigma_{ph}(\omega)$ and $\sigma(\omega)$ at the band edge implies direct photogeneration of separated charge carriers; no significant exciton binding energy is observed. The well-defined energy gap in stoichiometric $YBa_2Cu_3O_6$ is consistent with the electronic structure of a filled O $2p$ band located between the upper and lower Cu $3d$ Hubbard bands; the 1.5-eV feature determines the lowest interband transition. Doping of oxygen into the O(1) sites results in a major change in electronic structure. For $x \approx 0.3$, the absorption observed throughout the ir in $\sigma(\omega)$ has no counterpart in $\sigma_{ph}(\omega)$; the photoconductivity turns on near 2 eV. The photoconductive response and its temperature dependence demonstrate that the electronic states involved as either initial or final states in the transitions below 2 eV are localized.

II. EXPERIMENT

The c-axis epitaxial films (CuO_2 plane parallel to the substrate) of $YBa_2Cu_3O_{6+x}$ were made by laser ablation onto MgO or La_2AlO_3 substrates with *in situ* control of oxygen atmosphere; the films were post-annealed in Ar to yield the desired insulating compositions.[25] The growth conditions for the films were controlled to achieve the stoichiometric limit; the films studied had $x \approx 0$, as indicated by the clean transmission below 1.5 eV (described in detail below) and as proved by x-ray-diffraction measurements. The single crystals of $YBa_2Cu_3O_{6+x}$ are typically $0.5 \times 0.5 \times 0.1$ mm in size, and details on the preparation were published previously.[24] The oxygen concentration is near $x \approx 0.3$ with thermally activated dark conductivity in the ab plane at $T > 100$ K, $\rho(T) = \rho_0 \exp(E_a / k_B T)$, with $E_a \approx 0.18$–0.24 eV. X-ray-diffraction data from the crystals with $E_a \approx 0.2$ eV yield lattice parameters corresponding to $x \approx 0.3$.[14]

Photocurrent signals were detected by a computer controlled lock-in amplifier as a voltage drop across a load resistor, chosen properly at each test temperature to obtain the necessary sensitivity. The excitation light source was a tungsten halogen lamp dispersed by a grating monochromator equipped with proper order filters. The monochromatic beam was modulated by a mechanical chopper, then focused onto the photoconductive cell which is mounted in a vacuum chamber. A surface cell geometry was used; the crystal was placed on the center of a $\frac{1}{2}$ in. square alumina substrate with the ab plane parallel to the substrate, and 0.6-mm-wide gold electrodes were evaporated on the top surface with a gap of 0.2 mm (for epitaxial films, the electrodes were evaporated directly onto the top surface of the film). The final connection was made by bridging the electrodes with silver paste from the crystal to the substrate. In this arrangement, the charge carriers are excited and probed in the ab planes (CuO_2 planes). This cell was attached to the tip of a cryostat cold finger that allows measurements as a function of temperature. The field strength was 10^2–2×10^3 V/cm; in this range, the dark current was proportional to the voltage (i.e., ohmic).

The spectral resolution was set 2 nm at 2.5 eV, and the photon flux was about 0.4 mW/cm^2 at the same energy. To cancel out the spectral response of the measurement system, the photoconductive cell was replaced by a broadband pyroelectric detector (for use in the ir) or a calibrated photodiode (for use in the visible); the spectral response of the measurement system was then taken under identical conditions and used as the background for the normalization of the photoconductivity spectra. All photoconductivity measurements were made with samples in vacuum ($< 1 \times 10^{-4}$ Torr).

The reflectance, $R(\omega)$, of crystals of $YBa_2Cu_3O_{6.3}$ was measured by means of a photomodulation technique configured for reflectance at near-normal incidence (0.6–4 eV); the data were extended into the mid-ir (0.05–0.5 eV) with Fourier transform infrared instrumentation. The optical conductivity was obtained from $R(\omega)$ by a Kramers-Krönig transformation. For epitaxial films, the absorption and the reflectance were obtained with a Perkin-Elmer Lambda-9 spectrometer.

III. EXPERIMENTAL RESULTS

A. $YBa_2Cu_3O_{6.0}$ (epitaxial films)

The photoconductive response, $\sigma_{ph}(\omega)$, of a $YBa_2Cu_3O_{6.0}$ epitaxial film is plotted on a semilog scale in Fig. 1, along with the absorption spectrum $\alpha(\omega)$

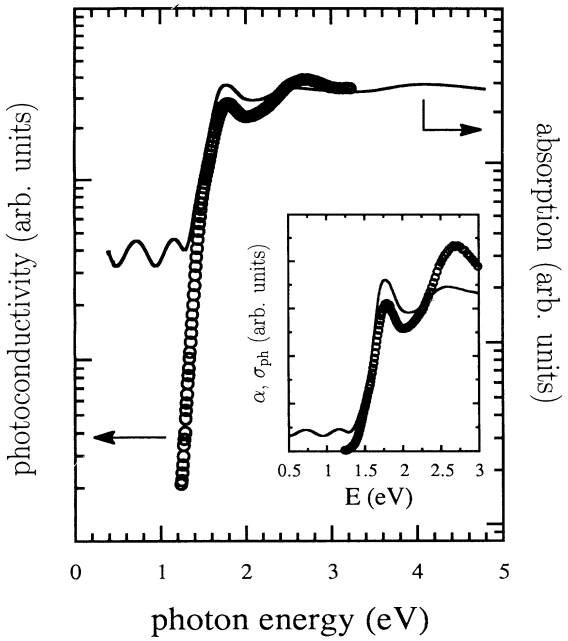

FIG. 1. The photoconductivity $\sigma_{ph}(\omega)$ in an $YBa_2Cu_3O_{6.0}$ epitaxial film (semilog scales) are compared with the absorption spectrum $\alpha(\omega)$; both spectra were taken at 300 K. The inset shows a linear plot in the vicinity of the band edge.

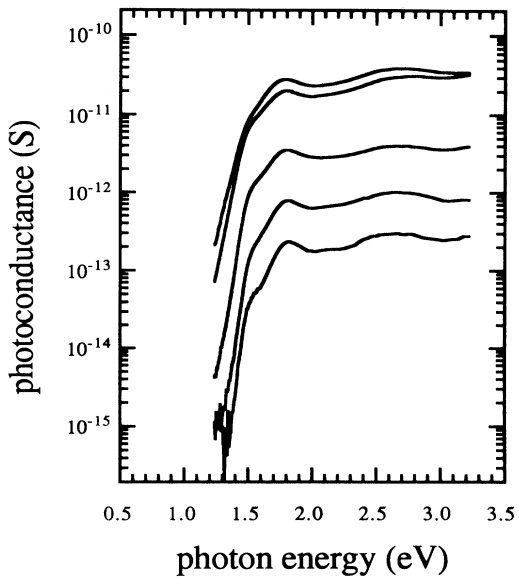

FIG. 2. The $\sigma_{ph}(\omega)$ in the same film as in Fig. 1 on semilog scale at several temperatures. The spectra are normalized to equal photon density of 10^{15} $cm^{-2}s^{-1}$. From top to bottom: 300, 220, 150, and 100 K. The lowest curve was taken on a different area of the same film at 81 K.

$=4\pi\sigma(\omega)/n(\omega)c$, where $n(\omega)$ is the real part of the complex index of refraction. Both spectra were obtained from the same film at 300 K. A linear plot in the vicinity of the band edge is shown in the inset. The absorption data in Fig. 1 were obtained by transmission measurements through the semitransparent thin films. The optical conductivity as obtained from $R(\omega)$ by the Kramers-Krönig relation is consistent with $\alpha(\omega)$ as measured by transmission (assuming Beer's law). The absorption spectrum in $YBa_2Cu_3O_{6+x}$, with $x \approx 0$ is characterized by three strong absorption features at 1.7, 2.7, and 4.2 eV, similar to that reported in the literature.[2,26–28] A clean energy gap (with no significant absorption) is implied by the nearly undamped oscillating structure in the ir due to multiple internal reflection.[29,30] Using $n \approx 2$ for the ir refractive index,[11] the period of the oscillation yields a thickness of 0.3 μm, consistent with the value estimated from the laser ablation conditions and from the absorption coefficient measured above the CT gap.[2,26,28]

In addition to the main features at 1.7 and 2.7 eV observed in $\alpha(\omega)$, a weak shoulder can be resolved in $\sigma_{ph}(\omega)$ centered at 1.5 eV (with a sharp slope change on both sides). In $\sigma(\omega)$ as measured either by transmission or reflectance, which weak 1.5-eV feature is barely detectable due to the oscillations from multiple internal reflection (for the reflectivity in single crystals, it is limited by the experimental sensitivity).[1,31]

In Fig. 2, the $\sigma_{ph}(\omega)$ data are plotted on a semilog scale for several temperatures (T) from 300 to 80 K; the features become sharper and easier to resolve at low temperatures. Although the 1.5-eV band is about five times weaker than the 1.7 and 2.7 eV bands, it is the lowest interband transition and determines the band edge. In fact, at 80 K, the photocurrent decreases by about two orders of magnitude within 0.1 eV below the peak. The sharp band edge and the T-independent ratio between the 1.5-eV band and the other two bands (1.7 and 2.7 eV) suggest that the 1.5-eV feature arises from an intrinsic interband transition. The weak slope change (below 1.5 eV) with temperature is due to the thermal broadening, as observed for the 1.7 and 2.7 eV bands.

The plateau in $\sigma_{ph}(\omega)$ around 2.1 eV at 300 K (see Fig. 1 and the top curve in Fig. 2) sharpens into a weak peak at low temperatures. Although this weak band has been observed in ellipsometry measurements[2,27,32] and in resonant Raman scattering,[10] it has received relatively little attention.

We have put considerable effort into verifying the existence of the 1.5-eV absorption band; in particular, to rule out the possibility of an artifact due to multiple internal reflections or due to sample quality. The results are summarized as follows:

(i) The multiple reflection data were analyzed from several different films with different thicknesses; the 1.5-eV feature was found in all cases. For example, for the data shown in Fig. 1 with oscillation maxima at 0.71 and 1.16 eV, the next interference maximum should be at 1.61 eV rather than at 1.5 eV.

(ii) By using the absorption formula for a thin film (with multiple reflections),[29] we have been able to separate the multiple reflections from the raw transmission data and thereby obtain a pure absorption spectrum. The feature at 1.5 eV can be seen in $\alpha(\omega)$, with a slope

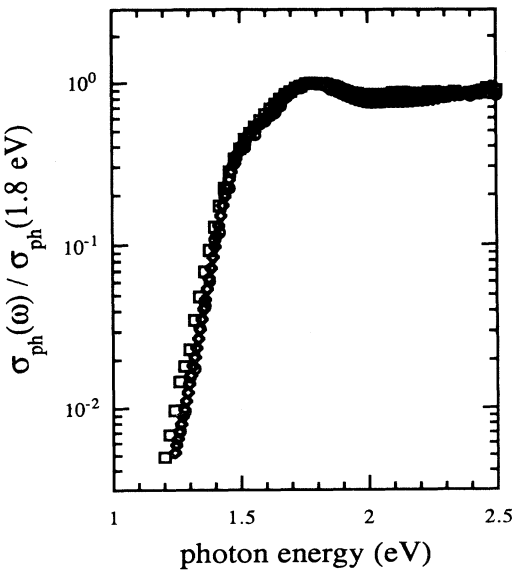

FIG. 3. The $\sigma_{ph}(\omega)$ from three epitaxial films of $YBa_2Cu_3O_{6.0}$ are compared. (◇) film *A* (0.3 μm in thickness) at 220 K, (□) film *B* (0.5 μm) at 200 K, (○) film *C* (0.6 μm) at 200 K.

change near 1.5 eV similar to that observed in $\sigma_{ph}(\omega)$, as shown in Figs. 1 and 2.

(iii) Four independent films from two batches with different thicknesses were measured. The $\sigma_{ph}(\omega)$ data from three of them (with thicknesses of 0.3, 0.5, and 0.6 μm, respectively) are shown in Fig. 3. The data are essentially identical to each other, independent of film thickness; the 1.5-eV feature is observed in all samples.

(iv) This 1.5-eV feature was also observed in $\sigma_{ph}(\omega)$ in partially doped single-crystal $YBa_2Cu_3O_{6.3}$ at low temperatures (see following section).

Based upon the spectra in Fig. 2, the temperature coefficients associated with each band can be obtained. To locate the peak energies more precisely, the data obtained at each temperature were fit to a superposition of four energy bands within Gaussian line shape. The peak

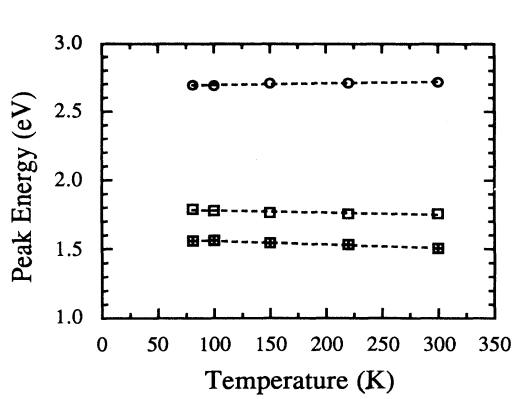

FIG. 4. Temperature dependences of the three main bands in $YBa_2Cu_3O_{6.0}$. (▦) 1.5 eV band, (□) 1.75 eV band, and (○) 2.7 eV band. The dashed lines are the results of linear fitting.

TABLE I. Peak energies and their corresponding temperature coefficients for $\sigma_{ph}(\omega)$ for stoichiometric $YBa_2Cu_3O_{6.0}$. $E(T)=E(0)+aT$.

E(300 K) (eV)	E(0 K) (eV)	a (eV/K)
1.51	1.59	-2.5×10^{-4}
1.75	1.79	-1.5×10^{-4}
2.71	2.68	$+1.1\times10^{-4}$

energies are then obtained from the fitting data. These results are plotted in Fig. 4. The zero-temperature energies of each band and the corresponding temperature coefficients can then be obtained from fitted curves (as shown in Fig. 4). The 1.5 and 1.7 eV bands are blue shifted upon cooling, while the 2.7-eV band is slightly red shifted on cooling. The peak energies at 300 and 0 K and the corresponding temperature coefficients obtained from the fitting data are summarized in Table I. These results, along with the results obtained under high pressure,[26] might prove useful in comparison with the band structure of $YBa_2Cu_3O_{6.0}$ calculated from various theoretical models.

B. $YBa_2Cu_3O_{6.3}$ (single crystals)

The single crystals of $YBa_2Cu_3O_{6.3}$ used for this study are from the same batches used for transient photoexcitation experiments;[12,14,24] the thermal activation energies of the resistivity ranged from 0.18 to 0.24 eV.

As is well known, adding oxygen to the O(1) sites in $YBa_2Cu_3O_{6+x}$ results in a rapid increase of oscillator strength in the subgap regime.[1,3,33] In Fig. 5 we plot $\sigma(\omega)$ for $YBa_2Cu_3O_{6.3}$; the *ab* plane $\sigma_{ph}(\omega)$ is plotted for the same crystal for comparison (both data sets were taken with the sample at 300 K). For the Kramers-Krönig transformation of $R(\omega)$, a constant value was used to extend the data below 0.05 eV, and the data of Tajima *et al.* (4–40 eV)[34] were used for the high-energy extension. The resulting $\sigma(\omega)$ data are similar to those published by other groups for samples with similar dopant concentration.[26]

The $YBa_2Cu_3O_{6.3}$ crystals are insulating; the dark conductivity is 2×10^{-3} S/cm at 300 K and $\sim10^{-11}$ S/cm at 100 K, with activation energy $E_a\approx0.24$ eV. Nevertheless, there is no energy gap in $\sigma(\omega)$ at this doping level. There is oscillator strength distributed over the entire ir, with $\sigma(\omega)$ having a magnitude comparable to that above 1.5 eV.

Detailed information on the excitations near the CT gap has been obtained from the temperature dependence. In Fig. 6 $\sigma_{ph}(\omega)$ is plotted for data obtained at 340, 300, 240, and 190 K [the data are normalized to σ_{ph} (2.5 eV)]. The results are quite different from those obtained from $YBa_2Cu_3O_{6.0}$ (Figs. 1 and 2); in $YBa_2Cu_3O_{6.3}$, $\sigma_{ph}(\omega)$ decreases rapidly for $\hbar\omega<2.1$ eV, where the optical conductivity remains large. In addition, the peak at 1.7 eV in $\sigma_{ph}(\omega)$ becomes strongly temperature dependent. At 300 K, σ_{ph} (1.7 eV) is about an order of magnitude lower than at 2.7 eV; the 1.7-eV band shows up only as a shoulder (see Fig. 5). Moreover, this magnitude drops by

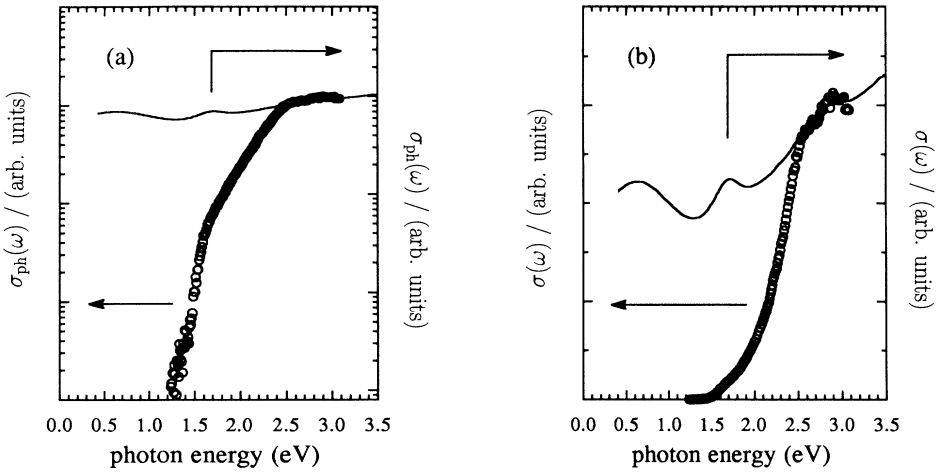

FIG. 5. Photoconductivity, $\sigma_{ph}(\omega)$, in a single crystal of $YBa_2Cu_3O_{6.3}$, compared with the optical conductivity $\sigma(\omega)$; (a) semilog scale, (b) on linear scale. Both spectra were taken at 300 K.

about a factor of 10 when the sample is cooled from 300 to 190 K, and the shoulder at 1.7 eV nearly disappears. This strong temperature dependence is observed only in $\sigma_{ph}(\omega)$; there is no corresponding temperature dependence in $\sigma(\omega)$.[35]

Above 2.1 eV, the profile of $\sigma_{ph}(\omega)$ (Fig. 6) is insensitive to temperature; i.e., the photocarriers excited with photon energies larger than 2.1 eV have a common thermal activation energy for transport. The value of this thermal activation energy is similar to that of dark conductivity, which is a measure of the energy interval between the Fermi energy and the mobility edge.[14,36]

In the range from 1.4 to 2.1 eV, $\sigma_{ph}(\omega)$ is weaker than that at 2.7 eV, and the profile is strongly dependent on temperature; the lower the photon energy, the stronger the dependence. This effect is shown in the inset of Fig. 6, in which the temperature dependence of $\sigma_{ph}(\omega)$ is plotted for several photon energies; the increase of the thermal activation energy with decreasing photon energy for $\hbar\omega < 2.1$ eV is clear. This behavior implies that the carriers photoexcited into this energy range require additional thermal energy to contribute to the photoconductivity, evidence that the electronic states involved in these transitions are localized. Therefore, the spectral gap in the $\sigma_{ph}(\omega)$ in Fig. 5 corresponds to the mobility gap in $YBa_2Cu_3O_{6.3}$. The photoconductive response at energies below 1.5 eV is very weak, and the magnitude becomes less sensitive to temperature below 240 K.

The chopping frequency (Ω) dependence of $\sigma_{ph}(\omega)$ in crystals of $YBa_2Cu_3O_{6.3}$ shows a power-law dependence $\sigma_{ph} \approx \Omega^{\beta}$, with β in the range of 0.55–0.65 for several samples. To explore the response under long-time illumination, $\sigma_{ph}(\omega)$ was also measured under steady-state light illumination at 300 K.[29] In this measurement, the light was switched by a computer-controlled shutter, and the time response of $\sigma_{ph}(\omega)$ at each wavelength was obtained in the following sequence of steps: (i) switch the light onto the sample, and record the time dependence of the current increase until it reaches steady state; (ii) switch the light off, and record the decay until the current reaches the initial dark value.

The steady state σ_{ph} is defined as the difference between the saturated value under illumination and the initial dark value. Generally, a period of 300–500 s is required for σ_{ph} to saturate, and 500–2000 s for σ_{ph} to relax back to the initial dark value. The decay of σ_{ph} is nonexponential. The profile of $\sigma_{ph}(\omega)$ measured under steady-state conditions is similar to that measured at 10 Hz, except the 1.7-eV band is slightly enhanced.[29]

The 1.5-eV feature is also observed in $\sigma_{ph}(\omega)$ for

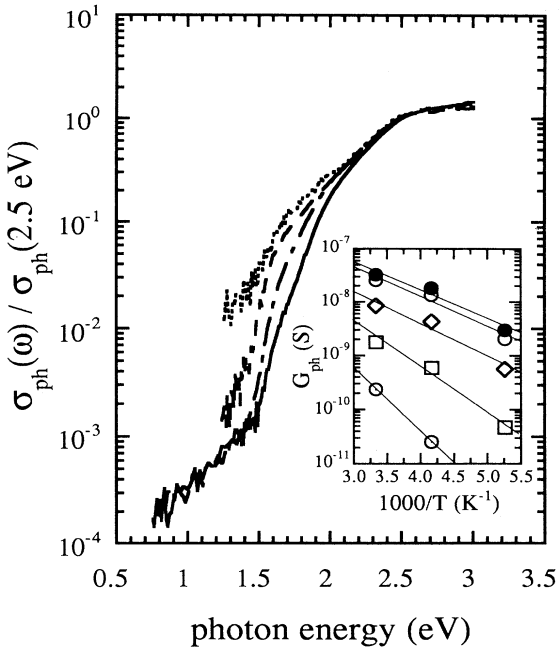

FIG. 6. The $\sigma_{ph}(\omega)$ in $YBa_2Cu_3O_{6.3}$ normalized to $\sigma_{ph}(2.5$ eV) at several temperatures; from top to bottom: 340, 300, 240, 190 K. In inset, the photoconductance G_{ph} at several photon energies are plotted against $1/T$ (under photon flux of 10^{15} $cm^{-2}s^{-1}$); (●) 3.0 eV, (○) 2.5 eV, (◇) 2.1 eV, (□) 1.8 eV, and (⊙) 1.4 eV. The E_a of the G_{ph} is enhanced for photon energy less than 2 eV.

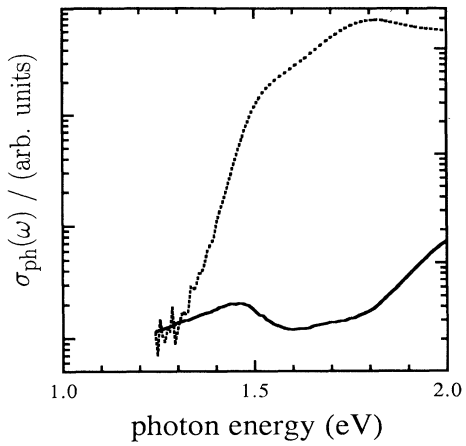

FIG. 7. The $\sigma_{ph}(\omega)$ in crystal $YBa_2Cu_3O_{6.3}$ (solid line) and in $YBa_2Cu_3O_{6.0}$ film (dashed line) at 100 K.

$YBa_2Cu_3O_{6.3}$ at temperatures below 150 K. In Fig. 7 the $\sigma_{ph}(\omega)$ data of single-crystal $YBa_2Cu_3O_{6.3}$ are plotted and compared with $\sigma_{ph}(\omega)$ for a $YBa_2Cu_3O_{6.3}$ film. Both spectra were taken at 100 K. Note that the data in Figs. 5, 6, and 7, are from the same crystal. More than eight crystals have been measured, with similar results for all the crystals with $E_a > 180$ meV. Thus, the 1.5-eV feature exists in a broad oxygen range ($0 \leq x \leq 0.3$). Although the states involved in transitions below 2 eV are localized in $YBa_2Cu_3O_{6.3}$ [at 100 K, σ_{ph} (1.5 eV) is still two to three orders of magnitude lower than σ_{ph} (2.6 eV)], the 1.5-eV feature appears as a small peak at temperatures below 150 K, while it is not resolvable at temperatures above 190 K (see Figs. 5 and 6).

The 1.5-eV feature was also recently observed in Raman experiments of $YBa_2Cu_3O_{6+x}$ and Nd_2CuO_{4-x} under UV laser excitation;[37] the Raman mode has A_{2g} symmetry. Crystal symmetry requires that the same feature cannot be visible in both Raman and absorption spectroscopies (and thus photoconductivity) in pure $YBa_2Cu_3O_{6.0}$. This fact suggests that some symmetry-breaking mechanism is in operation which enables the transition to be visible in both spectroscopies. The simplest mechanism for breaking the local symmetry is polaron formation.

IV. DISCUSSION

A. Photoconductive response in $YBa_2Cu_3O_{6.0}$: A Mott-Hubbard insulator with a *CT* energy gap

The $\sigma_{ph}(\omega)$ and $\sigma(\omega)$ results in Figs. 1 and 2 provide a clear picture of an insulator with a well-defined energy gap; there is no absorption for $\hbar\omega < 1.5$ eV. Since $\sigma(\omega)$ is proportional to the joint density of states, the clean spectral gap seen in both $\sigma_{ph}(\omega)$ and $\sigma(\omega)$ in Fig. 1 indicates that there are no states within the charge-transfer gap in stoichiometric $YBa_2Cu_3O_{6.0}$; the top of the O $2p$ band lies 1.5 eV below the bottom of the Cu $3d$ upper Hubbard band (UHB). Moreover, the coincidence of the $\sigma_{ph}(\omega)$ and $\sigma(\omega)$ spectral profiles in $YBa_2Cu_3O_{6.0}$ implies that photoabsorption at the CT gap results in mobile carriers rather than neutral excitons.

One of the initial motivations of this study was to identify whether the 1.7-eV feature is due to a neutral exciton, since the initial data obtained from partially doped $YBa_2Cu_3O_{6.3}$ indicated that this absorption band does not contribute to the photoconductivity at intermediate doping levels (verified in detail in Fig. 6).[24] Our results in $YBa_2Cu_3O_{6.0}$ rule out this possibility, since the strongest tendency toward excitonic binding must occur in undoped $YBa_2Cu_3O_{6.0}$ rather than in partially oxygen-doped $YBa_2Cu_3O_{6.3}$. In fact, in $YBa_2Cu_3O_{6.0}$ (Figs. 1 and 2), the 1.7-eV feature in $\sigma_{ph}(\omega)$ follows that in $\sigma(\omega)$; it has a similar magnitude to that at 2.7 eV. The overall behavior of the 1.7-eV feature is similar to that observed for the bands at 1.5, 2.1, and 2.7 eV (e.g., the ratio of the magnitudes is nearly temperature independent, etc.). Thus the 1.7 eV absorption results in separated charges rather than neutral excitons. Similar results have been observed in $La_2CuO_{4+\delta}$ and in $Nd_2CuO_{4-\delta}$ at low doping concentrations.[38,39]

A temperature-dependent shoulder, 0.2 eV below the CT gap, was recently observed in La_2CuO_4 at low temperatures (by reflectance).[40] This was attributed to a bound exciton which was assumed to thermally dissociate at higher temperatures. However, no corresponding temperature dependence is observed in the 1.5-eV structure in $YBa_2Cu_3O_{6.0}$ (see Fig. 2), nor in $Nd_2CuO_{4-\delta}$ in a similar energy range.[39] Further studies of the shoulder in the La_2CuO_4 system (for example, with crystals at different dopant concentrations) are needed to sort out these apparent differences.

Although band-structure calculations can explain many aspects of the electronic structure of superconducting $YBa_2Cu_3O_{7-\delta}$,[2,7-9] they fail to predict that stoichiometric $YBa_2Cu_3O_{6.0}$ is an antiferromagnetic insulator. The origin of this discrepancy is understood; the strong correlations of the Cu(2) d electrons are not adequately included in the local-density approximation.[10] On the other hand, the three-band Hubbard model[41] (based upon the σ-bonded orbitals, O(2) p_x, O(3) p_y, and Cu(2) $d_{x^2-y^2}$) correctly predicts both the energy gap and the antiferromagnetic ordering. Based upon this model, the electronic structure of $YBa_2Cu_3O_{6.0}$ is that of a Mott-Hubbard insulator, but with the lowest optical gap resulting from charge transfer. The Cu $d_{x^2-y^2}$ band (possibly hybridized with the O p_x and p_y orbitals) is split by the on-site Coulomb repulsion U_d into an unoccupied upper Hubbard band (UHB) and an occupied lower Hubbard band (LHB). The occupied oxygen band lies between the UHB and LHB, separated from the UHB by an energy gap E_g. This gap is determined by the charge-transfer energy Δ, and the p-d hopping matrix element t in the form of $E_g \approx 2\sqrt{\Delta^2 - 4t^2}$ (Ref. 41). In this sense, the undoped $YBa_2Cu_3O_{6.0}$ is often called a charge-transfer insulator (e.g., Ref. 1) with an energy gap of the order of Δ.

Resonance Raman-scattering data provide an effective method to identify which atoms in the lattice contribute to specific energy bands.[42] This analysis has been carried

out for stoichiometric $YBa_2Cu_3O_{6.0}$.[10] The results indicate that the optical transitions at 1.7, 2.1, and 2.7 eV are all due to in-plane CT excitations from oxygen bands to the upper Hubbard band. However, it is not clear at present whether these peaks are due to critical points in the Brillouin zone and/or to different interband transitions (e.g., from the two O p_x or p_y bands to the Cu $3d$ UHB).

B. Photoconductive response in $YBa_2Cu_3O_{6.3}$: Evidence of a Fermi glass

In contrast to $YBa_2Cu_3O_{6.0}$, the optical spectroscopy and photoconductivity of $YBa_2Cu_3O_{6.3}$ demonstrate that at intermediate doping levels, the electronic structure is that of a Fermi glass. In partially doped $YBa_2Cu_3O_{6.3}$, the strong peak in $\sigma(\omega)$ at 1.7 eV indicates that the joint density of states involved in this transition remains relatively large, although oscillator strength shifts to below the CT gap as a result of the chemical doping (see Fig. 5). The weak $\sigma_{ph}(\omega)$ below 2 eV demonstrates that carriers in the initial and final states involved in these low-energy transitions have low mobility; i.e., they are localized.

The strong temperature dependence found for $\sigma_{ph}(\omega)$ at 1.7 eV provides additional evidence that the states associated with this transition are localized. As in lightly doped $Nd_2CuO_{4-\delta}$,[39] the spectral edge in $\sigma_{ph}(\omega)$ of $YBa_2Cu_3O_{6.3}$ measures the mobility gap which is about 2.1 eV. Photocarriers excited by low-energy photons ($\hbar\omega < 2.1$ eV) require additional thermal energy to contribute to conduction. This implies that these carriers are initially excited into localized states which are not far from the mobility edge. At sufficiently high temperatures, the photocarriers (holes) can be thermally excited to the extended states across the mobility edge and thus can contribute to the conductivity.

Similar phenomena have been reported recently in the photoconductive response of C_{60} and/or C_{70} films.[43] In fact, a similar scheme was proposed to describe the photoconductive response of amorphous silicon, the prototype disordered semiconductor.[44] A common feature among these systems is that the thermal activation energy of the excited carriers is insensitive to the photon energy above the mobility gap; while the thermal activation energy increases for photon energies below the mobility gap; the lower the photon energy, the higher the thermal activation energy (see the inset of Fig. 6).

We note that there are a variety of data which support the conclusion that the electronic structure at intermediate doping levels is that of a Fermi glass. The variation of the exponent β in the power-law decay of the transient photoconductivity, $\sigma_{ph}(t) \approx t^{-(1-\beta)}$, in the same materials[13,14,45] implies a common physical origin for the two phenomena, i.e., thermally activated conduction in a Fermi glass insulator. In the infrared, one finds no structure in $\sigma_{ph}(\omega)$ corresponding to the broad 0.6-eV absorption band [the $\sigma_{ph}(\omega)$ data are restricted to $\hbar\omega > 0.62$ eV], suggesting that this doping-induced band is associated with states which are localized at $x \approx 0.3$. The nonexponential time decay of σ_{ph} after prolonged illumination, the chopping frequency dependence, and the steady-state $\sigma_{ph}(\omega)$ are also consistent with the Fermi glass energy structure. Details will be presented in a separate paper.[29]

There have been reports of photoconductive response in epitaxial films of insulating $YBa_2Cu_3O_{6+x}$.[46,47] The results in Ref. 46 are qualitatively similar to the data in partially doped single-crystal samples presented in this paper (the oxygen content in those films may be lower). The response curve in Ref. 47 is similar to that of undoped $YBa_2Cu_3O_{6.0}$, although the oxygen content in those films was suggested to be close to $x = 0.4$. Since no absorption spectra were taken *in situ* in these films, and since the oxygen in thin films is unstable, decreases with time, and finally approaches $x \approx 0$,[14,47] the uncertainties of the oxygen concentration in these films may account for the difference between these spectra.

C. Change of the electronic structure by oxygen doping

The experimental results reported in Figs. 1–7 provide direct information on the electronic structure and the nature of the electronic states in $YBa_2Cu_3O_{6+x}$ at different oxygen doping levels. The mobility gap in the electronic structure can be identified by photoconductive response experiments. Figure 8 shows $\sigma_{ph}(\omega)$ at three different oxygen levels in insulating $YBa_2Cu_3O_{6+x}$ ($0 < x < 0.4$); the spectral gap in $\sigma_{ph}(\omega)$ shifts toward higher proton energy with oxygen doping. The sharp decrease of the $\sigma_{ph}(\omega)$ at the 2.1-eV band in samples near the MI transition, and the high oscillator strength in the infrared at this doping level indicate that the electronic states involved in the 0.6-. 1.5-, and 1.7-eV transitions are localized in $YBa_2Cu_3O_{6+x}$ for $x \approx 0.3$–0.4.

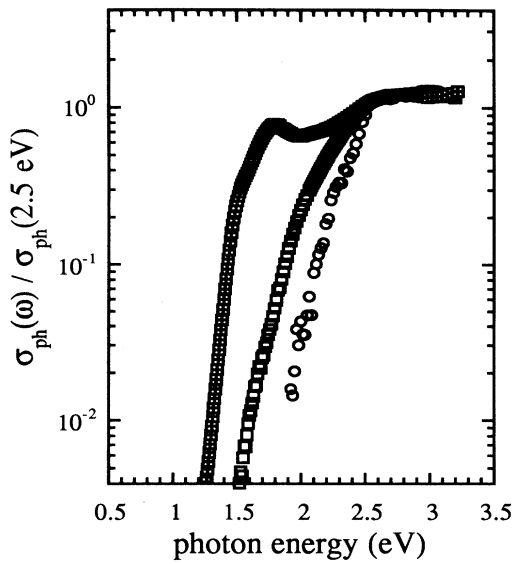

FIG. 8. Photoconductive responses in $YBa_2Cu_3O_{6+x}$ at three different oxygen levels: (□) in $YBa_2Cu_3O_{6+x}$ with $x \to 0$, (□) in $YBa_2Cu_3O_{6.3}$ with $\rho_{300\ K} \approx 500\ \Omega$ cm and $E_a \approx 0.24$ eV, and (○) in $YBa_2Cu_3O_{6+x}$ with $\rho_{300\ K} \approx 100\ \Omega$ cm and $E_a \approx 0.1$ eV ($0.3 < x < 0.4$).

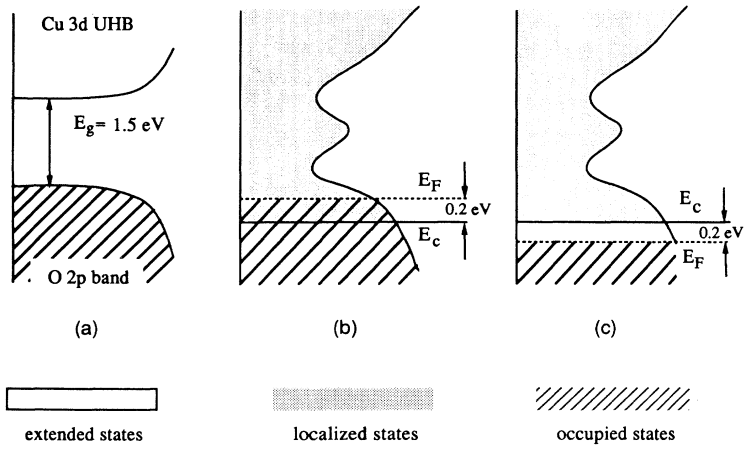

FIG. 9. The proposed electronic structure of $YBa_2Cu_3O_{6+x}$: (a) stoichiometric $YBa_2Cu_3O_{6.0}$, (b) partially doped insulating $YBa_2Cu_3O_{6.3}$, and (c) doped metallic $YBa_2Cu_3O_{6+x}$ with $x \approx 1$.

The activation energy of the dark conductivity in a Fermi glass insulator is a measure of the energy difference between E_F (which lies in the regime of localized states) and E_c. Adding oxygen into the lattice removes electrons from the CuO_2 planes, resulting in a shift of E_F into the O $2p$ band and across E_c, thereby inducing the MI transition. This is supported by experimental evidence from photoemission and electron energy-loss spectroscopies which shows that the holes in $YBa_2Cu_3O_7$ are introduced into the O $2p$ band.[48–50]

Based on these experimental results, the electronic structure of $YBa_2Cu_3O_{6+x}$ can therefore be sketched for three doping levels, $x=0$, $x=0.3$, and x, close to but less than 1, as shown in Fig. 9. The corresponding positions of E_F and E_c are indicated for each doping level. The diagram in Fig. 9(a) ($x=0$) corresponds to an insulator with a CT energy gap between the O $2p$ band and the Cu $3d$ UHB, the diagram in Fig. 9(b) ($x \approx 0.3$), corresponds to a Fermi glass insulator with E_F in the region of localized states, and the diagram in Fig. 9(c) ($x \approx 1$) corresponds to the metallic phase with optimized superconductivity where E_F is in the origin of extended states, but relatively close to the mobility edge.

Using the measured density of states near E_F in $YBa_2Cu_3O_7$ (10^{22} states/eV cm^3),[51] the carriers introduced by oxygen doping from $x \approx 0.4$ (at the MI transition where $E_F = E_c$) to $x \approx 1$ (0.6 carriers per formula) will fill states in an energy interval of approximately 0.2 eV from the mobility edge, consistent with the experimental observations.[52] Thus, the electronic structure of the high-T_c metallic regime is like that shown in Fig. 9(c); $E_F \approx 0.2$ eV below E_c, lying in the extended-state region in the O $2p$ band.

V. CONCLUSION

In conclusion, critical comparison of the photoconductive response and the optical conductivity in insulating $YBa_2Cu_3O_{6+x}$ ($x < 0.4$) has enabled us to monitor the evolution of the electronic structure from that of a Mott-Hubbard insulator with a charge-transfer energy gap to that of a Fermi glass. Stoichiometric $YBa_2Cu_3O_{6.0}$ is a Mott-Hubbard insulator with a CT gap between the O $2p$ band and the Cu $3d$ UHB. Oxygen doping leads to a random distribution of oxygen ions at O(1) sites; the doping process adds carriers (holes) to the CuO_2 planes, causing a shift in oscillator strength from the interband transition to energies below the charge-transfer gap and simultaneously causes localization of the electronic states near the Fermi level. The MI transition occurs at doping levels sufficiently high that the Fermi energy shifts into the regime of O $2p$ band and across the mobility edge. The proximity of E_F to E_c (with E_F in the O $2p$ band) in the metallic HTSC cuprates is a situation which is rather special and might therefore be a feature of special relevance to the existence of high-temperature superconductivity.[53]

ACKNOWLEDGMENTS

We thank Professor D. J. Scalapino for important comments, Dr. G. Z. Zhang for taking $R(\omega)$ in the range of 0.05–0.5 eV, L. Smilowitz, Khashayar Pakbaz, and T. Hagler for help with a variety of experimental problems. This work is supported by the National Science Foundation (NSF DMR91-21946).

*Permanent address: Jozef Stefan Institute, University of Ljubljana, Ljubljana, Jamova 39, Slovenia.

[1] J. Orenstein, G. A. Thomas, A. J. Millis, S. L. Cooper, D. H. Rapkine, T. Timusk, L. F. Schneemeyer, and J. V. Waszczak, Phys. Rev. B **42**, 6342 (1990), and references therein.

[2] J. Kircher, M. K. Kelly, S. N. Rashkeev, M. Alouani, D. Fuchs, and M. Cardona, Phys. Rev. B **44**, 217 (1991), and references therein.

[3] D. B. Tanner and T. Timusk, in *Physical Properties of High-Temperature Superconductors III*, edited by D. M. Ginsberg (World Scientific, Singapore, 1992), p. 363.

[4] R. Feile, Physica C **159**, 1 (1989).

[5] K. Kitazawa and S. Tajima, *Some Aspects of Superconductivity* (Nova Science, New York, 1990).

[6] C. Thomsen and M. Cardona, in *Physical Properties of High-Temperature Superconductors I*, edited by D. M. Ginsberg (World Scientific, Singapore, 1989), p. 409.

[7] E. T. Heyen, S. N. Rashkeev, I. I. Mazin, O. K. Anderson, R.

Liu, M. Cardona, and O. Jepsen, Phys. Rev. Lett. **65**, 3048 (1990).
[8]W. E. Pickett, Rev. Mod. Phys. **61**, 433 (1989).
[9]O. K. Anderson, Physica C **185-189**, 147 (1991).
[10]E. T. Heyen, J. Kircher, and M. Cardona, Phys. Rev. B **45**, 3037 (1992).
[11]For example, G. A. Thomas, D. H. Rapkine, S. L. Cooper, S-W. Cheong, A. S. Cooper, L. F. Schneemeyer, and J. V. Waszczak, Phys. Rev. B **45**, 2474 (1992).
[12]G. Yu, C. H. Lee, A. J. Heeger, N. Herron, and E. M. McCarron, Phys. Rev. Lett. **67**, 2581 (1991).
[13]G. Yu, C. H. Lee, A. J. Heeger, S-W. Cheong, and Z. Fisk, Physica C **190**, 563 (1992).
[14]G. Yu, C. H. Lee, A. J. Heeger, N. Herron, E. M. McCarron, L. Cong, G. C. Spalding, C. A. Nordman, and A. M. Goldman, Phys. Rev. B **45**, 4964 (1992).
[15]S. Tanda, M. Honma, and T. Nakayama, Phys. Rev. B **43**, 8725 (1991).
[16]D. Mandrus, L. Forro, C. Kendziora, and L. Mihaly, Phys. Rev. B **44**, 2418 (1991).
[17]N. W. Preyer, R. J. Biegeneau, C. Y. Chen, D. R. Gabbe, H. P. Jessen, M. A. Kastner, P. J. Picone, and T. Thio, Phys. Rev. B **39**, 11 563 (1989); P. Lunkenheimer, M. Resch, A. Loidl, and Y. Hidaka, Phys. Rev. Lett. **69**, 498 (1992).
[18]S. J. Hagen, J. L. Peng, Z. Y. Li, and R. L. Greene, Phys. Rev. B **43**, 13 606 (1991).
[19]C. Y. Chen, R. J. Birgeneau, M. A. Kastner, N. W. Preyer, and T. Thio, Phys. Rev. B **43**, 392 (1991).
[20]P. Lunkenheimer, M. Resch, A. Loidl, and Y. Hidaka, Phys. Rev. Lett. **69**, 498 (1992).
[21]C. M. Rey, H. Mathias, L. R. Testardi, and S. Skirius, Phys. Rev. B **45**, 10 639 (1992).
[22]G. A. Samara, W. F. Hammetter, and E. L. Venturini, Phys. Rev. B **41**, 8974 (1990).
[23]R. Raffaelle, H. U. Anderson, D. M. Sparlin, and P. E. Parris, Phys. Rev. B **43**, 7991 (1991).
[24]G. Yu, A. J. Heeger, G. Stucky, N. Herron, and E. M. McCarron, Solid State Commun. **72**, 345 (1989).
[25]C. Fincher (unpublished).
[26]M. Garriga, U. Venkateswaran, K. Syassen, J. Humlicek, M. Cardona, H. Mattausch, and L. Schonher, Physica C **153-155**, 643 (1988); S. L. Cooper, D. Reznik, A. Kotz, M. A. Karlow, R. Liu, M. V. Klein, W. C. Lee, J. Giapintzakis, and D. M. Ginsberg, Phys. Rev. B **47**, 8233 (1993).
[27]M. K. Kelly, P. Barboux, J.-M. Tarascon, D. E. Aspnes, W. A. Bonner, and P. A. Morris, Phys. Rev. B **38**, 870 (1988).
[28]H. Yasuoka, H. Mazaki, T. Terashima, and Y. Bando, Physica C **175**, 192 (1991).
[29]G. Yu, C. H. Lee, and A. J. Heeger (unpublished).
[30]A. Yariv, *Optical Electronics* (Saunders College Publishing, Philadelphia, 1991).
[31]S. L. Cooper, G. A. Thomas, J. Orenstein, D. H. Rapkine, M. Capizzi, T. Timusk, A. J. Millis, L. F. Schneemeyer, and J. V. Waszczak, Phys. Rev. B **40**, 11 358 (1989).
[32]A. L. Kotz, M. V. Klein, W. C. Lee, J. Giapintzakis, D. M. Ginsberg, and B. W. Veel, Phys. Rev. B **45**, 2577 (1992).
[33]T. Timusk and D. B. Tanner, in *Physical Properties of High-Temperature Superconductors I,* edited by D. M. Ginsberg (World Scientific, Singapore, 1989), p. 339.
[34]S. Tajima, H. Ishii, T. Nakahashi, T. Takagi, S. Uchida, M. Seki, S. Suga, Y. Hidaka, M. Suzuki, T. Murakami, K. Oda, and H. Unoki, J. Opt. Soc. Am. B **6**, 475 (1989).
[35]G. A. Thomas (private communication).
[36]N. F. Mott and E. A. Davis, *Electronic Processes in Non-Crystalline Materials* (Clarendon, Oxford, 1979).
[37]R. Liu, M. V. Klein, D. Salamon, S. L. Cooper, W. C. Lee, S-W. Cheong, and D. M. Ginsberg, J. Chem. Phys. Solids (to be published).
[38]T. Thio, R. J. Birgeneau, A. Cassanho, and M. A. Kastner, Phys. Rev. B **42**, 10 800 (1990).
[39]G. Yu, C. H. Lee, A. J. Heeger, and S-W. Cheong, Physica C **203**, 419 (1992).
[40]J. P. Falck, A. Levy, M. A. Kastner, and R. J. Birgeneau, Phys. Rev. Lett. **69**, 1109 (1992).
[41]C. A. Balseiro, M. Avignon, A. G. Rojo, and B. Alascio, Phys. Rev. Lett. **62**, 2624 (1989); V. J. Emery, *ibid.* **58**, 2794 (1987).
[42]M. Cardona, in *Light Scattering in Solids II,* edited by M. Cardona and G. Guntherodt (Springer-Verlag, Berlin, 1982).
[43]M. Kaiser, J. Reichenbach, H. J. Byrne, J. Anders, W. Maser, S. Roth, A. Zahab, and P. Bernier, Solid State Commun. **81**, 261 (1992).
[44]In *Semiconductors and Semimetals,* edited by R. K. Willardson and A. C. Beer (Academic, New York, 1984), Vol. 21.
[45]G. Yu and A. J. Heeger, Int. J. Mod. Phys. B (to be published).
[46]R. Boyn, K. Lobe, H.-U. Habermeier, and N. Prub, Physica C **181**, 75 (1991).
[47]C. Ayache, I. L. Chaplygin, A. I. Kirilyuk, N. M. Kreines, and V. I. Kudinov, Solid State Commun. **81**, 41 (1992).
[48]A. Fujimori, E. Takayama-Muromachi, Y. Uchida, and B. Okai, Phys. Rev. B **35**, 8814 (1987).
[49]N. Nucker, J. Fink, J. C. Fuggle, P. J. Durham, and W. M. Temmerman, Phys. Rev. B **37**, 5158 (1988).
[50]N. Tucker, H. Romberg, X. X. Xi, J. Fink, B. Gegenheimber, and Z. X. Zhao, Phys. Rev. B **39**, 6619 (1989).
[51]B. Batlogg, Physica B **169**, 7 (1991).
[52]D. R. Harshman and A. P. Mills, Phys. Rev. B **45**, 10 684 (1992), and references therein.
[53]A. J. Heeger and G. Yu, Phys. Rev. B **48**, 6492 (1993).